

Article

# Process and Formulation Strategies to Improve Adhesion of Nanoparticulate Coatings on Stainless Steel

Jutta Hesselbach <sup>\*</sup>, Ann-Christin Böttcher, Ingo Kampen, Georg Garnweitner <sup>id</sup>, Carsten Schilde and Arno Kwade <sup>id</sup>

Institute for Particle Technology, Technische Universität Braunschweig, 38106 Braunschweig, Germany; ann-christin.boettcher@tu-braunschweig.de (A.-C.B.); i.kampen@tu-braunschweig.de (I.K.); g.garnweitner@tu-braunschweig.de (G.G.); c.schilde@tu-braunschweig.de (C.S.); a.kwade@tu-braunschweig.de (A.K.)

\* Correspondence: jutta.hesselbach@tu-braunschweig.de; Tel.: +49-531-3-91-9613

Received: 19 January 2018; Accepted: 21 April 2018; Published: 26 April 2018



**Abstract:** The use of ceramic nanoparticles in coatings can significantly improve their mechanical properties such as hardness, adhesion to substrate, and scratch and abrasion resistance. A successful enhancement of these properties depends strongly on the coating formulation used, and the subsequent structure formed during coating. The aim of the present work was to enhance the adhesion between nanoparticulate coatings and stainless-steel substrates. A covalent particle structure was formed and better mechanical properties were achieved by modifying alumina nanoparticles, as well as substrates, with 3-aminopropyltriethoxysilane and by using a formulation consisting of solvent, modified particles, and bisphenol-A-diglycidylether as cross-linking additive. In addition to the adhesion force needed to remove the coating from the substrate, the type of failure (adhesive or cohesive) was characterized to gain a deeper understanding of the structure formation and to identify interdependencies between process, formulation, and coating structure properties. The modification process and the formulation composition were varied to achieve a detailed conception of the relevant correlations. By relating the results to other structural properties, such as the theoretical porosity and thickness, it was possible to understand the formation of the coating structure in more detail.

**Keywords:** alumina; nanoparticles; cross-linking; formulation; coating adhesion

## 1. Basics and State of the Art

Nanoparticulate coatings are commonly employed to mechanically enhance the surface properties of a variety of materials as well as to achieve self-cleaning effects [1–3]. The properties of such coatings do not only depend on the materials of the coating, but are also strongly influenced by the respective structural characteristics. The final coating structure and, thus, the final coating properties, are defined by a variety of parameters for every single process step. For this reason, our group has already focused in recent works on the investigation of the effect of process and formulation parameters along the whole process chain on the properties of nanoparticle-based coatings [4–8]. Based on these previous works, the aim of the present study was to achieve better mechanical properties, especially concerning the adhesion of thin nanoparticulate coatings to the substrate using a combination of modified particles and modified substrates, as it is schematically displayed in Figure 1a. The modification of the particles was performed in a similar fashion as in [9], while the modification of the substrates was done by a simple dip-coating process in solutions of the modification agent 3-aminopropyltriethoxysilane (APTES), which is referred to as the ligand throughout this study. In general, other research groups have shown how to bond various materials to a solid substrate [10–14]. However, the aim of most works was to

achieve monolayers and the procedure to prepare the substrates seems to be time intensive. Therefore, our goal was to improve the coating adhesion technique using this easy-to-implement procedure. The amino groups of the ligand react with the epoxy groups of the additive (bisphenol-A-diglycidylether) at higher temperatures. The use of this formulation strategy has already shown the potential to increase the hardness and scratch resistance of nanoparticulate alumina coatings by cross-linking primary particles and aggregates [8]. Additionally, as it is displayed in Figure 1b, the amount of abrasion used as a reference value for abrasion resistance, as well as the adhesion between the coatings and unmodified substrates, could be enhanced. Different methods are described in the literature [15–17] to characterize the adhesion of a film onto a substrate. In this study, we decided to measure the adhesion force  $F_A$ —which is the force needed to remove the coating from the substrate by means of a stamp—following a well-established procedure (according to the pull-off test for adhesion ISO 4624:2003 [18]).

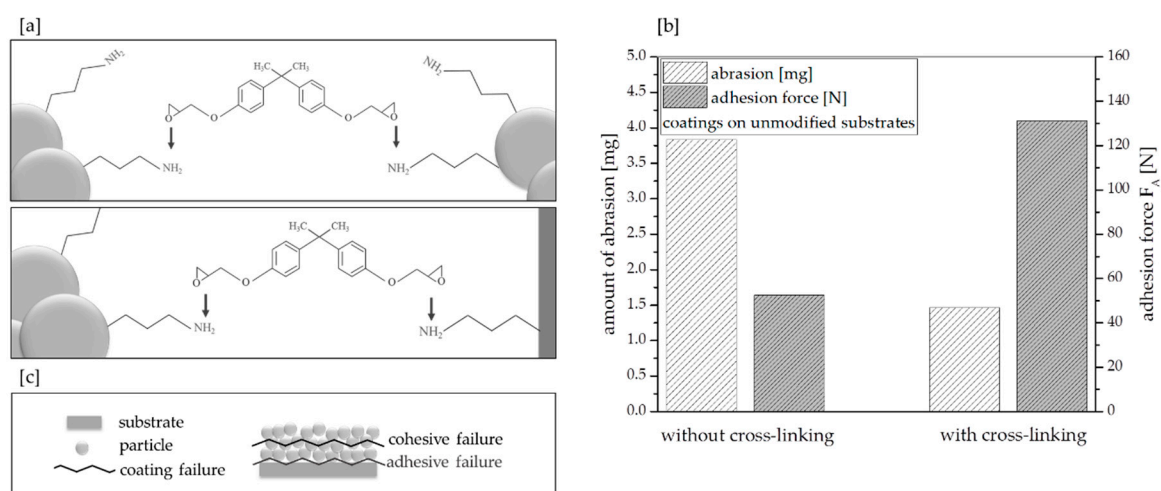


**Figure 1.** Cross-linking between particles as well as between particle and modified substrate (a); amount of abrasion and adhesion force of coatings with and without cross-linking (b); kind of failure during adhesion measurement (c).

Complementary to previous research, the particles used in the present study can cross-link to each other and can also be attached to the substrate by the modification shown in Figure 1a. Dependencies between the used formulation, the particulate structure, and the coating properties were investigated in detail in order to identify important relationships. Additionally, the kind of failure was also distinguished. As it is schematically shown in Figure 1c, the failure mechanisms can be classified into cohesive and adhesive failures. On the one hand, cohesive failure occurs within the coating and is therefore related to the inner strength of the coating. On the other hand, adhesive failure takes place at the interface between the coating and the substrate and is thus associated to the strength of the bonds formed between both materials. In fact, cohesive failure can take place in the case that the coordination number between the particles is small or the bond forces within the particulate structure are weak. With the help of these investigations, we were able to acquire a deeper understanding about the structure formation and how the substrate modification process and the formulation parameters influence the coating properties.

## 2. Materials and Methods

As it is shown in Figure 2, the process chain consists of four steps, and their experimental setups are explained in the following sections.

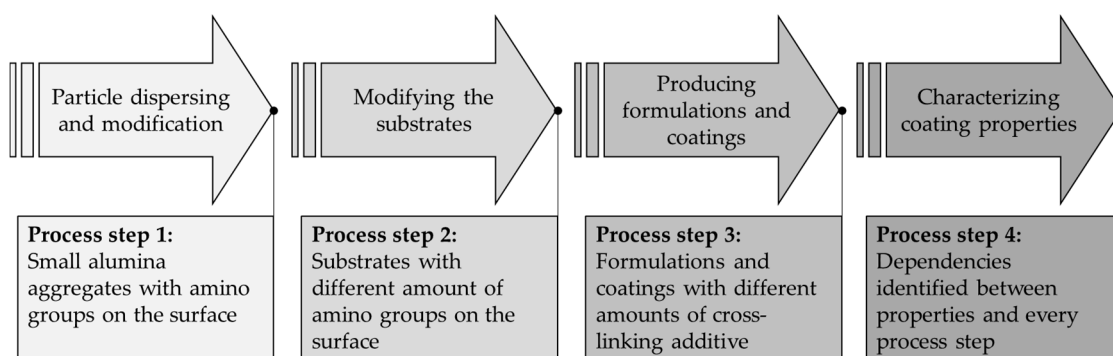


**Figure 2.** Process chain to produce covalently linked particle coatings on modified substrates.

### 2.1. Step 1: Modifying the Substrates

The dip-coating process (Coater Model idLab) was used to modify the substrates. Polished stainless-steel substrates were coated with an APTES–ethanol solution, with an APTES-content of 10 wt %. The ethanol was technical grade, APTES was purchased from the company Sigma Aldrich (St. Louis, MO, USA, assay 98%), and liquids were mixed at room temperature. Various process speeds (50, 100, 200, 300, and 500 mm/min) were used to achieve different wet film thicknesses, thus various amounts of APTES were used on the substrates. As it is well known, according to Landau and Levich [19], the wet film thickness increases with higher coating speed. The substrates were dried at 120 °C for 2 h and then used in the subsequent coating step (Step 3). The amount of APTES was determined by measuring the amount of silicon using energy dispersive X-ray spectroscopy (QX 400, Bruker, Billerica, MA, USA). For this study, the amount of silicon was related to the silicon content that was detected on the stainless-steel substrates without undergoing any modification (0.89 at % Si). The determined contents for the different samples are shown in Table 1. It can be observed that the values for the coating speeds of 50 and 100 mm/min are very similar. A reason for this fact could be that the film was not very homogenous at these low speeds.

**Table 1.** Measured amounts of silicon on the substrates by varying the process speed in the modification step.

Coating Speed $v$ (mm/min)	Amount of Silicon (at %)
50	1.17
100	1.23
200	1.46
300	2.26
500	2.71

### 2.2. Step 2: Particle Dispersing and Modification

In principle, the materials and methods used within this work are similar to the study shown in [8], but additional methods were introduced regarding the measurement of adhesion force and the characterization of cohesive and adhesive failure.

As the nanoparticle material, we used alumina nanoparticles (Evonik, Essen, Germany) with a primary particle size of 13 nm according to the data sheet. To achieve smaller aggregate sizes, the nanoparticles were suspended in technical ethanol with a solid content of 10 wt %, stabilized with nitric acid and dispersed for 4–5 h under 250 rpm using a planetary ball mill (Retsch, Haan, Germany) with a filling ratio of 30% (zirconia beads,  $d_{GM} = 300 \mu\text{m}$ ). The modification step with APTES (Sigma Aldrich) follows the dispersing step and was carried out overnight, as it is described in [8,9]. The particle sizes were determined using dynamic light scattering (Nanophox, Sympatec,

Clausthal-Zellerfeld, Germany) and the amount of APTES bound to the particle surface was examined by thermogravimetric analysis (Mettler Toledo TGA/DSC, Greifensee, Switzerland, under oxygen flow in the range of 25–700 °C). At the end of this first process step, the particles were finely dispersed ( $x_{50.3} \approx 150$  nm) in ethanol with amino groups on their surface. To ensure enough suspension for both series of experiments (substrates with different amount of ligand (Section 3) and variation of cross-linking additive concentration (Section 4)), this process step was carried out twice, one batch corresponding to one series.

### 2.3. Step 3: Producing the Formulations and Coatings

In order to achieve a cross-linking of the particles within the coatings, an additive had to be added to the dispersed and modified particles (see Step 2). Different concentrations of the additive bisphenol-A-diglycidylether were dissolved in ethanol and then added to the prepared suspension of particles to achieve various ratios of epoxy to amino groups in the coating formulations. The substrates with and without modification were coated with these nanoparticulate formulations ( $c_{m,particles} = 0.1$ ) via dip coating (Coater Model idLab) and with a constant coating speed of 500 mm/min. A commonly known interference measurement setup was used to characterize the wet film thickness for selected samples, similar to the setup described by Schmidt-Hansberg et al. [20]. Most of the solvent evaporates during the first minutes directly after the coating step. High temperatures are required to finally cross-link the particles to each other. For this reason, the coated substrates were tempered afterwards at 120 °C for 2 h.

### 2.4. Step 4: Characterizing Coating Properties

Several methods were used to characterize the coating structure as well as the structure properties. To determine the thickness of the nanoparticulate film, the coatings were scratched with an instrument made of brass and an applied force of about 1.9 N. In that way, the coating was partially removed but the substrate was not damaged, which was proved in preliminary works by EDX measurements. The resulting height difference was measured by a profilometer (Dektak, Bruker) using a diamond tip with a radius of 5 µm. Due to its small value, it was impossible to measure the thickness of the dried APTES-film. The determined mechanical properties of the coating structure are the adhesion force between substrate and coating and the hardness. The latter was examined via nanoindentation (TI900, Hysitron, Inc., Eden Prairie, MN, USA) using a Berkovich tip and measuring the maximal force by displacement-controlled measurements ( $l_{displ.} = 150$  nm). For statistic reasons, the measurement was repeated 40 times per sample to approach a constant value for the standard deviation of the measurement, as it was already established in other preliminary works [4,21,22]. The mean maximal force was related to the theoretical contact area of the tip to calculate the hardness. The measurement setup to characterize the adhesion force is based on a material testing machine (RetroLine, Zwick, Ulm, Germany) and follows DIN EN ISO 4624 [18]. It consists of a stamp ( $A = 100$  mm<sup>2</sup>) prepared with a testing tape (double-sided tape, Tesa 4968), which at first is moved from its starting position with  $v = 0.05$  mm/min onto the sample surface. Subsequently, the stamp is held at this position for 60 s with a contact pressure of  $F = 240$  N and then it is displaced back to the starting position with a higher velocity of  $v = 200$  mm/min. The force that is needed to tear off the coating is measured with the help of the software testXpert II (Zwick) and corresponds to the value of the so-called adhesion force  $F_A$ . The measurement was repeated three times per sample and the mean value and standard deviation were calculated. To characterize the kind of failure (cohesive or adhesive failure (see Figure 1c) the remaining amount of alumina was analyzed by detecting the aluminum left on the sample using energy dispersive X-ray spectroscopy (QX 400, Bruker). The abrasion resistance was characterized by stressing the surface with two abrading wheels (CS 10-F, TaberAbraser, Erichsen, Hemer, Germany) for a constant number of cycles, three times per sample. The amount of abrasion was determined gravimetrically and is a measure for the abrasion resistance. The picture of the cross-section was made with a FIB-SEM (focused-ion-beam-scanning-electron microscope, company FEI Deutschland

GmbH (now Thermo Fisher Scientific, Waltham, MA, USA), model: Helios G4 CX). For the sample preparation, the coating surface was sputtered with a platinum layer of 15 nm (High Vacuum Coater Leica EM ACE600, Wetzlar, Germany) to be electrically conductive. Before making a vertical cut in the coating by the ion beam, additional platinum was applied locally by a gas injection system with a height of about 1.5  $\mu\text{m}$  to protect the surface. In the first FIB step, a current of 2500 pA was used to remove the coarse material. Afterwards, the generated cut was polished in several steps. The last polishing step was done with a current of 40 pA.

### 3. Results

#### 3.1. Effect of Substrates with Different Amount of Modification Ligand

In order to investigate the process strategy for the substrate modification, the substrates were modified with the same APTES–ethanol solution but processed with various coating speeds to achieve different wet film thicknesses and thus various ligand concentrations on the substrate surfaces. Figure 3 shows an exemplary cross-section of a coating with modified nanoparticles and cross-linking additive on a stainless-steel substrate, which was modified with the maximum coating speed ( $v = 500 \text{ mm/min}$ ). The picture, obtained with a FIB-SEM, clearly presents each layer. In light of this image, it is clear why it is not possible to determine the thickness even for the maximum content of APTES.

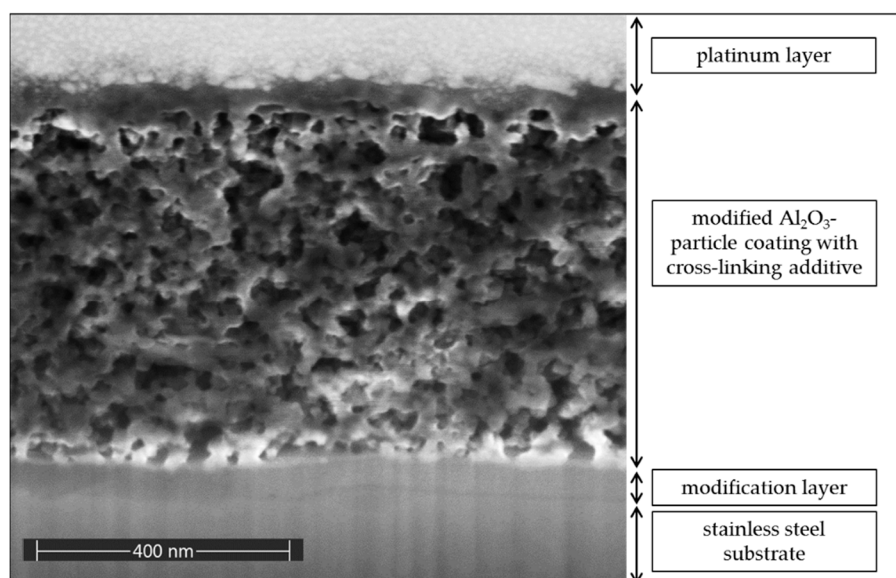


**Figure 3.** Cross-section of a coating on modified stainless-steel substrate.

In order to compare the use and non-use of cross-linking additive and to investigate the influence of the substrate modification on the coating properties, both kinds of formulations were prepared for the following coating step. The amount of ligand on the particle surface was 5.7 wt % and the ratio of  $N_{\text{epoxy}}/N_{\text{amino}}$  (number of epoxy groups of additive related to number of amino groups on the particle surface of ligand) in the used formulation was set constant to 1.5. The results in Figure 4 show the measured adhesion forces  $F_A$  as well as the remaining aluminium content (Al at %) as a value for the amount of alumina particles after tearing off the coatings for the experiments without using a cross-linking additive. Figure 4a shows that coatings without cross-linking have nearly the same adhesion force, especially if the moderate values of standard deviations are considered. However, it can be stated that the calculated mean adhesion force slightly decreases with increasing amounts of ligand on the substrates.

Furthermore, it can be observed that there is always remaining aluminum on the substrate after tearing off the coatings, which indicates a cohesive failure. However, it is directly perceived that the cohesive failure decreases by using substrates with increasing silicon amount.

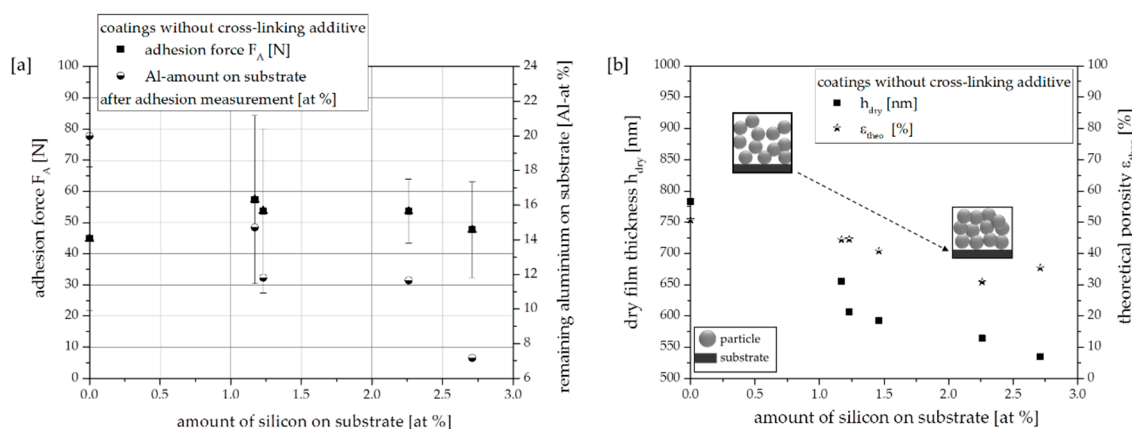


**Figure 4.** Coatings without cross-linking additive: measured adhesion forces and remaining aluminium on the substrate (a); dry film thickness and theoretical porosity (b).

A dominant tendency towards cohesive failure occurs if the coatings are thicker and have higher porosities and, thus, lower values of the particle coordination number without any change in particle interaction. Because of different substrate surface effects caused by the modification process, the wet film thickness cannot be calculated by the model of Landau and Levich [19]. For this reason, we measured the wet film thickness and related the determined values to the measured dry film thickness to calculate the theoretical porosity (described in [5]). Figure 4b shows that both dry film thickness and porosity are reduced for higher ligand amounts on the substrate. A closer packing of the coating structure with a higher coordination number between the particles ( $k_{pp} \gg 1$ ) induces greater strength at larger bond forces within the structure. The coordination number to the substrate is  $k_{ps} = 1$  and, therefore, the number of bonds to the substrate is smaller than the number of bonds within the coating, which enhances adhesion failure. Consequently, this kind of structure, combined with a low coating thickness, can result in smaller adhesion forces and a higher tendency towards adhesive failure, because it is easier to remove the film completely.

Nevertheless, the results after adding the cross-linking additive to the nanoparticulate formulations (hence, forming a structure involving covalent binding) do not reveal this trend, as it is displayed in Figure 5. Despite a higher standard deviation, it is clearly visible that the adhesion forces increase with higher amounts of modification ligand on the substrate. Additionally, the remaining amount of aluminium is nearly negligible, meaning that an adhesive failure takes place, with the exception of the coating on the unmodified substrate. In contrast to the conclusions made for the coatings without cross-linking, Figure 5b shows that both the dry film thickness and the theoretical porosity do not show a clear trend and thus are not significantly influenced by the surface modification for cross-linked coatings. In this case, the force required to remove the coating from the substrate is higher, even though the coatings are thicker on modified substrates with higher amount of ligand, in contrast to what has been stated before. Moreover, the higher porosity should not lead to higher adhesion forces and adhesive failures, as was found when using the cross-linking additive, because a high porosity is related to a lower coordination number within the coating and not at the interface to the substrate.

The reason for reaching higher adhesion forces is the modified and cross-linked particle structure, which translates into a much better binding degree to the substrate. Moreover, it must be remarked that, apart from the fact that the pull-off force is greater, the whole covalently bound particle structure

is removed completely from the substrate because of the chemically cross-linked particle network formation. This appears to be obvious, since the coordination number of the particles to the substrate is equal to 1 ( $k_{ps} = 1$ ) and the coordination number between particles is higher ( $k_{pp} \gg 1$ ). Furthermore, in the literature it has already been stated that during the drying process, small binder molecules can undergo segregation, resulting in an enrichment at the surface of the coatings [23], and that this mechanism feature induces lower adhesion to the substrate. Looking at non-cross-linked coatings on substrates without modification (Figure 4a), the adhesion force of the cross-linked coatings is higher in general, but there are also remaining alumina particles on the substrate after stressing the coating on the unmodified substrate, which means that the failure is cohesive. This failure within the structure could be due an analogous effect of an additive (cross-linker) demixing process in the structure, which probably leads to more strongly bound particles only in the upper part of the coating structure (schematically shown in Figure 5b) and results in a more cohesive failure in the lower part of the coating. The modification of the substrates might be effective against such a demixing of additive molecules, and thus the use of APTES-modified substrates could counteract this segregation effect.

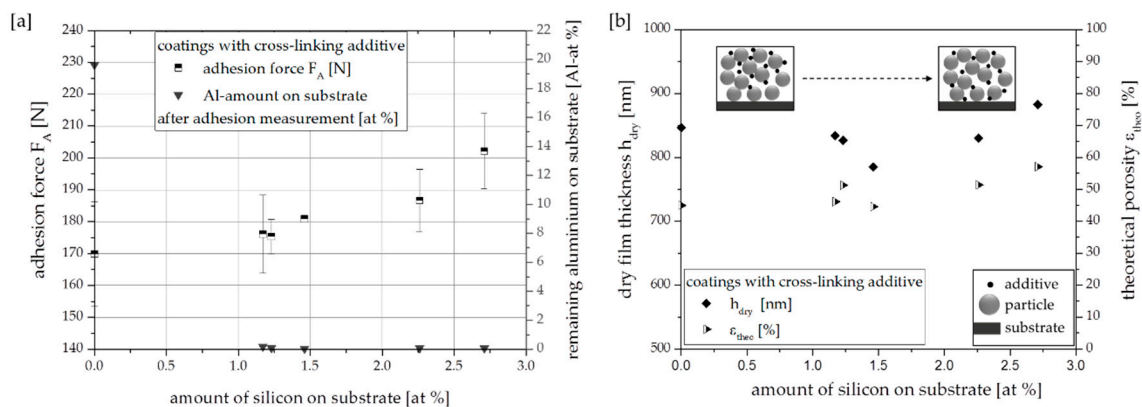


**Figure 5.** Coating with cross-linking additive: measured adhesion forces and remaining aluminium on substrate (a); dry film thickness and theoretical porosity (b).

In order to conclude these first investigations regarding the influence of the substrate modification process, we determined that using the modified substrates in combination with cross-linked particles induces greater adhesion between the particulate structure and the substrate. In-depth research to understand how the properties of the structure are influenced and how the coating behaves in failure has shown that the non-cross-linked structures are weaker within the film, which induces a cohesive failure. In contrast, using an additive in the coating formulation to cross-link the particles leads to adhesive failure because of stronger bindings and a higher coordination number between the particles compared to that of particles and substrate. The next section shows the results regarding the influence of the amount of cross-linking additive in the coating formulation on the properties described above, using a constant ligand concentration on the substrates.

### 3.2. Effect of Cross-Linking Additive Concentration

The aim of the second part of this research was to investigate how the adhesion between coating and substrate can be influenced by the formulation composition. Within this framework, formulations with different additive concentrations were used to coat substrates with and without modification. The amount of ligand on the particle surface in this series was about 6.9 wt % and the ratio of epoxy (cross-linking additive) to amino groups (particle surface modification) was varied between 0 and 2.5. Substrates without and with modification (3 at % of silicon,  $v_{mod.} = 500$  mm/min) were used to have detailed insight regarding these influencing parameters.

In general, the coatings on unmodified substrates exhibit cohesive failure, which has also been observed in Section 3, except for the coating with a  $N_{\text{epoxy}}/N_{\text{amino}}$  ratio of 1.5, which shows a lower amount of remaining aluminum on the substrate. This could be induced by a combination of smaller dry film thickness (about 100 nm less than the other coatings), which means a higher coordination number between the particles, and probably a better cross-linked structure. As a result, this coating needs a lower force to be removed from the substrate.

As expected, using substrates with APTES modification and cross-linking additive in the formulation leads to higher adhesion forces. Using additive ratios  $N_{\text{epoxy}}/N_{\text{amino}}$  between 0 and 1.5 and modified substrates leads to cohesive failure under the chosen experimental conditions. This cohesive failure is a reasonable result of a less cross-linked particle network within the coating structure. The coordination number between the particles  $k_{\text{pp}}$  is higher than between particles and substrate  $k_{\text{ps}}$ , but the binding to the substrate is preferred because of a larger contact area (noncovalently bound coating of the modification agent APTES). Additionally, taking into consideration the assumption made previously—that a substrate modification might act against a demixing effect with the additive molecules being classified in the upper coating area—the additive molecules only remain in the part of the coating in close proximity to the substrate when smaller amounts of additive are utilized, which ultimately leads to a cohesive failure (see schematic pictures in Figure 6b). The number of covalent bonds between the particles induced by the cross-linking additive rises using a  $N_{\text{epoxy}}/N_{\text{amino}}$  ratio of over 1.5. Under these circumstances, there are enough additive molecules, which are held to the substrate and are able to cross-link the particles within the whole films. The strength within the coating increases and fewer particles remain on the substrate after the testing procedure. For this reason, high additive concentrations in the coating formulations ( $N_{\text{epoxy}}/N_{\text{amino}} = 2\text{--}2.5$ ) cause an adhesive failure on the modified substrates, as was expected and observed before. However, the impact of the modification on the adhesion forces becomes minimal at a higher additive concentration of  $N_{\text{epoxy}}/N_{\text{amino}} = 2.5$ . This could probably arise from the effect of a higher amount of additive acting additionally like glue, with stronger induced interactions between the particles and the substrate. If this supposition is taken into account, a covalently bound particle network within the coating would not necessarily result. As it was shown in [8], the strength within the chemically cross-linked coatings on unmodified substrates reaches a maximum and then decreases at high additive concentrations because of a kind of oversaturated state—which is caused by more bound additive—hence, the cross-linking between two particles is hindered.

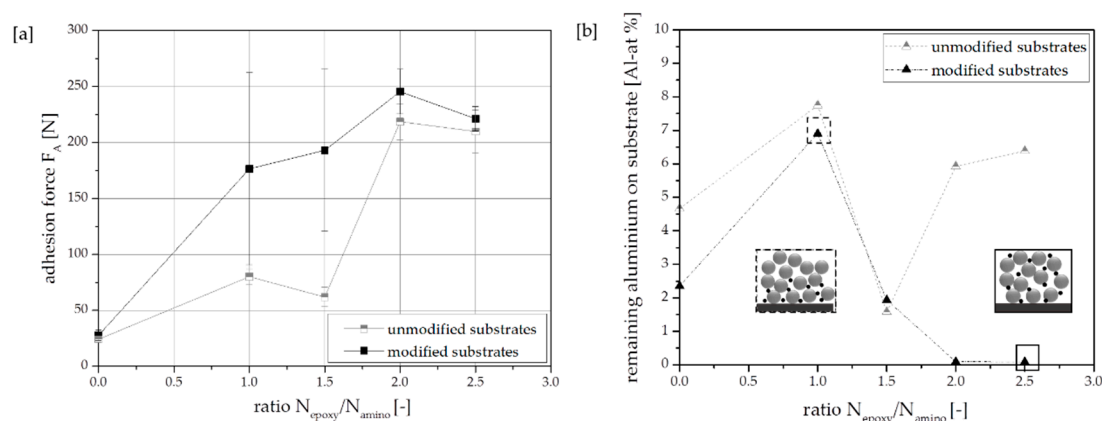


**Figure 6.** Measured adhesion forces (a) and remaining aluminium content (b) of coatings on unmodified and modified substrates.

This greater need for additive molecules to form a covalently bound particle network within the coating by using modified substrates can also be traced by measuring the hardness. As it has already been described in other studies [8], the hardness provides more information about the cross-linking

within the coating. The mentioned additive concentration optimum and oversaturated state can also be shown for the cross-linked coatings on unmodified substrates, as it is displayed in Figure 7a. The use of modified substrates leads to an increased amount of additive required for the binding between the coating and the substrate. As a result, the number of bonds within the coating is reduced, hence the hardness decreases for a given  $N_{\text{epoxy}}/N_{\text{amino}}$  ratio. The optimum ratio for the greatest hardness is probably shifted to higher additive concentrations, which should be investigated in further studies.

Besides the hardness and the adhesion, the abrasion resistance is another important mechanical property used to characterize particulate coatings. Figure 1b has already shown that the use of cross-linking of the particles leads to higher abrasion resistance on unmodified substrates. On account of the outcome presented in Figure 7b, it can be remarked that the additional use of modified substrates can successfully increase the abrasion resistance as well.

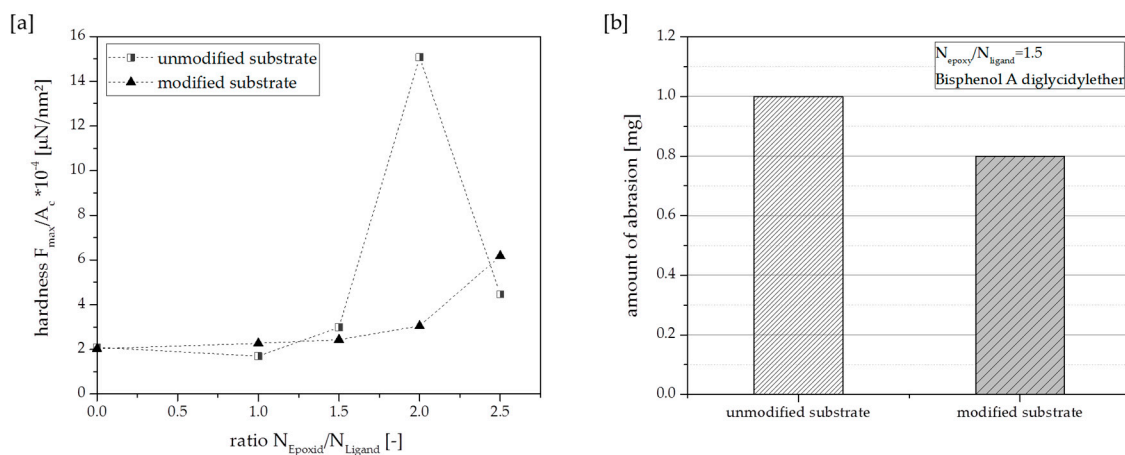


**Figure 7.** Hardness of coating on unmodified and modified substrates (a); amount of abrasion using unmodified and modified substrates (b).

#### 4. Conclusions

In the present study, stainless-steel substrates were modified by performing a dip-coating process in order to improve the adhesion between a particulate coating and the substrate by a chemical cross-linking. The mechanical properties are of special importance with regard to a variety of coating applications. Firstly, the influence of the amount of ligand on the substrate was investigated to provide a knowledge foundation. Secondly, the correlation between the amount of cross-linking additive in the coating formulation and the coating properties was established.

The obtained results led to several conclusions. Initially, it could be shown that the adhesion of particulate coatings on stainless-steel substrates can be enhanced by a modification process in combination with modified particles and the use of an additive to cross-link the structure. This substrate modification process was not complex and thus can be of special interest for industrial coating processes. Detailed investigations regarding the kind of failure caused by mechanically stressing the coatings and concerning the physical properties helped to develop a deeper understanding of how the structures are formed. This was achieved by varying the substrate properties and the formulation composition.

Essential relations between the formulation composition and the structure and properties of the coatings with different types of particle cross-linking were clarified by systematically studying the mentioned key parameters (amount of ligand on substrate and additive in formulation). Taking the presented outcomes into consideration, it is verified that a considerable improvement of the mechanical properties of thin coatings is feasible by adjusting the process and formulation parameters. Experiments were carried out to investigate the abrasion resistance for a ratio of  $N_{\text{epoxy}}/N_{\text{amino}} = 1.5$ . Besides the fact that the adhesion of the coatings was improved significantly, it could also be shown

that using the modified substrates had a positive effect on the abrasion resistance. The hardness of the coatings is greater at a ratio of epoxy to amino groups of  $N_{\text{epoxy}}/N_{\text{amino}} = 2$  by using unmodified substrates, whereas the use of modified substrates leads to a greater need for additive molecules, which probably changes the optimum additive concentration. This assumption has to be investigated in future work and should be proven by additional testing methods regarding the coating adhesion, such as scratch tests, as have been performed in previous research [8].

**Author Contributions:** Jutta Hesselbach performed and designed the main experiments, which were the basic for this study and interpreted the data in the way how it is shown in this study. Ann-Christin Böttcher assisted by a lot of experiments and by analyzing the data. She established and performed especially the method to characterize the kind of failure of the structured coatings. With the help of many years of experience and the base knowledge of Georg Garnweitner, Ingo Kampen, Carsten Schilde as well as Arno Kwade regarding modification of particles, structuring nanomaterials and characterizing the coating structures and properties, the results were interpreted finally and written down by Jutta Hesselbach in this manuscript.

**Acknowledgments:** This work was supported by the DFG (KW-9/16-2 and GA 1492/7-1, Project “Prozesskette-Eigenschafts-Beziehungen einer nanopartikulären Beschichtung”). The authors would also like to thank Stephanie Michel (iPAT, TU Braunschweig), Julia Stiller-Stuwe (iPAT, TU Braunschweig), Trung Thuong Duong (TU Braunschweig) and Clara Sangrós (iPAT, TU Braunschweig) who assisted in the measurements.

**Conflicts of Interest:** The authors declare that they have no conflict of interest.

## References

1. Kamegawa, T.; Shimizu, Y.; Yamashita, H. Superhydrophobic surfaces with photocatalytic self-cleaning properties by nanocomposite coating of TiO<sub>2</sub> and polytetrafluoroethylene. *Adv. Mater.* **2012**, *24*, 3697–3700. [[CrossRef](#)] [[PubMed](#)]
2. Yaghoubi, H.; Taghavinia, N.; Alamdari, E.K. Self cleaning TiO<sub>2</sub> coating on polycarbonate: Surface treatment, photocatalytic and nanomechanical properties. *Surf. Coat. Technol.* **2010**, *204*, 1562–1568. [[CrossRef](#)]
3. Lakshmi, R.V.; Bharathidasan, T.; Basu, B.J. Superhydrophobic sol-gel nanocomposite coatings with enhanced hardness. *Appl. Surf. Sci.* **2011**, *257*, 10421–10426. [[CrossRef](#)]
4. Barth, N.; Schilde, C.; Kwade, A. Influence of particle size distribution on micromechanical properties of thin nanoparticulate coatings. *Phys. Procedia* **2013**, *40*, 9–18. [[CrossRef](#)]
5. Barth, N.; Schilde, C.; Kwade, A. Influence of electrostatic particle interactions on the properties of particulate coatings of titanium dioxide. *J. Colloid Interface Sci.* **2014**, *420*, 80–87. [[CrossRef](#)] [[PubMed](#)]
6. Barth, N.; Zimmermann, M.; Becker, A.E.; Graumann, T.; Garnweitner, G.; Kwade, A. Influence of TiO<sub>2</sub> nanoparticle synthesis on the properties of thin coatings. *Thin Solid Films* **2015**, *574*, 20–27. [[CrossRef](#)]
7. Hesselbach, J.; Barth, N.; Lippe, K.; Schilde, C.; Kwade, A. Process chain and characterisation of nanoparticle enhanced composite coatings. *Adv. Powder Technol.* **2015**, *26*, 1624–1632. [[CrossRef](#)]
8. Hesselbach, J.; Kockmann, A.; Lüke, S.; Overbeck, A.; Garnweitner, G.; Schilde, C.; Kwade, A. Enhancement of the mechanical properties of nanoparticulate thin coatings via surface modification and cross-linking additive. *Chem. Eng. Technol.* **2017**, *40*, 1561–1568. [[CrossRef](#)]
9. Kockmann, A.; Hesselbach, J.; Zellmer, S.; Kwade, A.; Garnweitner, G. Facile surface tailoring of metal oxide nanoparticles via a two-step modification approach. *RSC Adv.* **2015**, *5*, 60993–60999. [[CrossRef](#)]
10. Basnar, B.; Litschauer, M.; Strasser, G.; Neouze, M.-A. Analyzing imidazolium bridging in nanoparticle networks covalently linked to silicon substrates. *J. Phys. Chem. C* **2012**, *116*, 9343–9350. [[CrossRef](#)]
11. Choi, S.Y.; Lee, Y.-J.; Park, Y.S.; Ha, K.; Yoon, K.B. Monolayer assembly of zeolite crystals on glass with fullerene as the covalent linker. *J. Am. Chem. Soc.* **2000**, *122*, 5201–5209. [[CrossRef](#)]
12. He, H.-X.; Zhang, H.; Li, Q.G.; Zhu, T.; Li, S.; Liu, Z.-F. Fabrication of designed architectures of au nanoparticles on solid substrate with printed self-assembled monolayers as templates. *Langmuir* **2000**, *16*, 3846–3851. [[CrossRef](#)]
13. Stratmann, M. Chemically modified metal surfaces—A new class of composite materials. *Adv. Mater.* **1990**, *2*, 191–195. [[CrossRef](#)]
14. Yoon, K.B. Organization of zeolite microcrystals for production of functional materials. *Acc. Chem. Res.* **2007**, *40*, 29–40. [[CrossRef](#)] [[PubMed](#)]
15. Hull, T.; Colligon, J.; Hill, A. Measurement of thin film adhesion. *Vacuum* **1987**, *37*, 327–330. [[CrossRef](#)]
16. Bull, S.J. Techniques for improving thin film adhesion. *Vacuum* **1992**, *43*, 517–520. [[CrossRef](#)]

17. Jacobsson, R. Measurement of the adhesion of thin films. *Thin Solid Films* **1976**, *34*, 191–199. [[CrossRef](#)]
18. DIN EN ISO 4624 Beschichtungsstoffe–abreißversuch zur beurteilung der haftfestigkeit; Deutsches Institut für Normung: Berlin, Germany, 2003.
19. Landau, L.; Levich, B. Dragging of a liquid by a moving plato. In *Dynamics of Curved Fronts*, 1st ed.; Pelce, P., Libchaber, A., Eds.; Academic Press: Cambridge, MA, USA, 2012; Volume 141.
20. Schmidt-Hansberg, B.; Klein, M.F.; Peters, K.; Buss, F.; Pfeifer, J.; Walheim, S.; Colsmann, A.; Lemmer, U.; Scharfer, P.; Schabel, W. In situ monitoring the drying kinetics of knife coated polymer-fullerene films for organic solar cells. *J. Appl. Phys.* **2009**, *106*, 124501. [[CrossRef](#)]
21. Barth, N.; Schilde, C.; Kwade, A. Einfluss von prozessparametern auf die mechanischen eigenschaften von nanopartikulären beschichtungen. *Chem. Ingenieur Tech.* **2012**, *84*, 328–334. [[CrossRef](#)]
22. Schilde, C.; Westphal, B.; Kwade, A. Effect of the primary particle morphology on the micromechanical properties of nanostructured alumina agglomerates. *J. Nanopart. Res.* **2012**, *14*, 745. [[CrossRef](#)]
23. Westphal, B.; Bockholt, H.; Günther, T.; Haselrieder, W.; Kwade, A. Influence of convective drying parameters on electrode performance and physical electrode properties. *ECS Trans.* **2015**, *64*, 57–68. [[CrossRef](#)]



© 2018 by the authors. Licensee MDPI, Basel, Switzerland. This article is an open access article distributed under the terms and conditions of the Creative Commons Attribution (CC BY) license (<http://creativecommons.org/licenses/by/4.0/>).